Scaling Massive MIMO Radar via Compressive Signal Processing

Maryam Eslami Rasekh*, Upamanyu Madhow†
University of California Santa Barbara
Email: {*rasekh, †madhow}@ece.ucsb.edu

***Abstract*—Massive MIMO radars that utilize many transmit and receive antennas can provide range extension and fine-grained angular resolution in sensing. Current signal processing strategies for MIMO radar impose a strict tradeoff between range and angular field of view, preventing efficient scaling to massive MIMO platforms. In this paper, we present a compressive signal processing framework to sidestep this tradeoff. Relying on the sparsity of the scene in angular domain, we take advantage of compressive beam scanning to provide high resolution direction estimates with a small number of beacons that scales logarithmically with array size. The proposed approach enables scaling to massive MIMO frontends while maintaining a small, almost constant frame interval, thereby facilitating high resolution direction estimation and range extension without sacrificing the field of view or imaging speed.**

***Index Terms*—CWFM radar, MIMO radar, compressive estimation, range extension, massive MIMO.**

I. Introduction

Utilizing many transmit and/or receive antennas enables a radar system to provide high-resolution direction information in addition to range and doppler, which is immensely beneficial to many applications such as environment awareness for autonomous vehicles, target classification, and close-range gesture recognition. Using a large number of transmit elements can also provide power combining gains and expand the sensing range and SNR. At mmWave and THz frequencies, massive MIMO frontends with hundreds or thousands of elements can fit on small platforms, and several prototypes have been built for communication applications until now [1]–[3]. By repurposing these frontends for sensing, the many benefits of massive MIMO radar can be realized.

Unfortunately, current signal processing strategies for MIMO radar impose a strict tradeoff between range and field of view that prevents efficient scaling to massive MIMO platforms. Conventional MIMO radar systems typically utilize time-interleaved sensing (for digital transmit arrays) or directional beam scanning (for digital or analog arrays) to obtain direction estimates [4], [5]. The frame structure of these two methods is depicted in Figure 1. In the former approach, transmitters take turns broadcasting chirp sequences and the received measurements are aggregated to emulate the full MIMO response. Since only one transmitter is active at any time, this method does not realize the full transmit power combining gain and range extension of MIMO. This is also true for the case of orthogonalizing transmitter signals in domains other than time as proposed in [6]. Furthermore, since the number of chirp bursts in each frame scales proportionally to array size, this strategy is not scalable to very large transmit arrays due to the limited coherence time of the scene. The beam scanning approach, on the other hand, utilizes the power combining gain of the array, but it too scales poorly to large arrays with narrow beams, as covering a large (fixed) field of view with narrow beams requires a number of chirp sequence transmissions that scales linearly with array size. Thus to allow sufficiently fast scanning, one must limit either the transmit array size (hence, range extension capacity) or the field of view that is scanned in each frame.

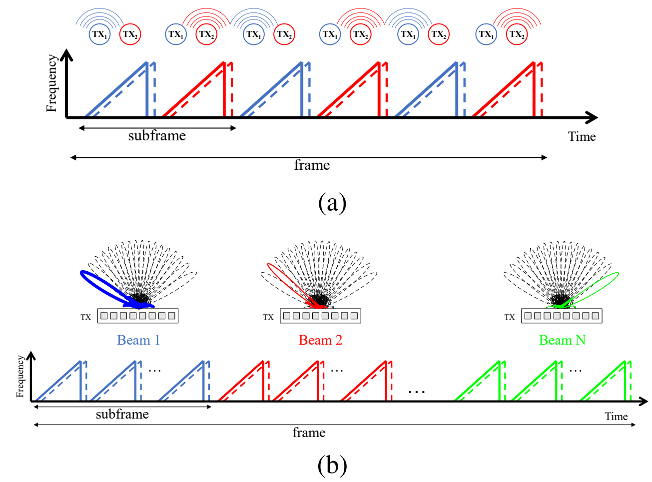

Fig. 1: Frame structure for (a) time-interleaved [4], (b) beamformed scanning [5] radar.

In order to circumvent these limitations, we propose an alternative approach that, relying on the angular sparsity of the scene in each range-doppler bin, takes advantage of compressive signal processing to provide high resolution direction estimates with a small number of subframes (chirp bursts) that scales *logarithmically* with array size. We borrow ideas from the extensive literature on compressive channel estimation for MIMO communication applications, and overlay compressive estimation in the spatial domain with the conventional range and Doppler estimation of continuous wave frequency modulated (CWFM) radar. Our numerical results show that with as few as 10 compressive beacons, target directions can be estimated with the full resolution of a 128-element transmit

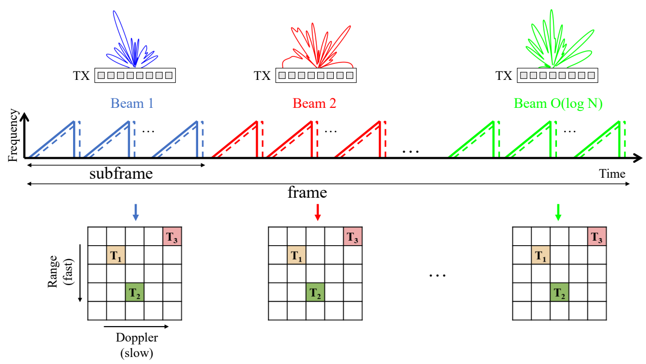

Fig. 2: Proposed frame structure for compressive radar.

aperture, providing an order of magnitude reduction in the frame size compared to beamformed scanning.

A. Related work

The wireless channel, especially at higher frequencies where massive MIMO frontends are feasible, consists of only a small number of paths and is therefore sparse in the spatial frequency domain. Thus, compressive channel estimation from a small number of random projections has been employed in communication applications for low-overhead channel tracking on large phased arrays with RF beamforming [7], [8]. Since the spatial frequency of each path lies on a continuum, conventional techniques for sparse vector estimation are not suitable for channel estimation. In [9], an algorithm is proposed for off-grid compressive estimation using orthogonal matching pursuit with Newton refinement of parameters between nullspace projections. As massive MIMO frontends are deployed for radar imaging, adapting the compressive signal processing techniques developed in communication literature to sensing platforms is increasingly of interest.

In sensing literature, "compressive" or "sparse" MIMO radar typically refers to one of two cases. In the first case, target sparsity in the angle-Doppler-range space is exploited to compress the received signal via a linear transformation, as discussed in [6], [10], [11]. These methods require transmit elements to transmit independent signals, and are therefore incompatible with the large RF-beamformed arrays that we propose to repurpose for sensing. The second case refers to random undersampling of the spatial domain, i.e., sparsity in terms of hardware realization wherein transmit and receive array elements are placed at random so that a large aperture is sampled compressively with fewer antenna elements [12]. In contrast, our focus here is on compressive sampling to take advantage of the sparsity of the scene in the *spatial frequency* domain, which allows us to observe the entire field of view with fewer beams than would be required by beamformed scanning. We note that the two concepts are complementary: compressive sampling in spatial frequency domain using large transmit arrays, as proposed here, can be combined with randomly spaced receive antennas to efficiently synthesize large apertures.

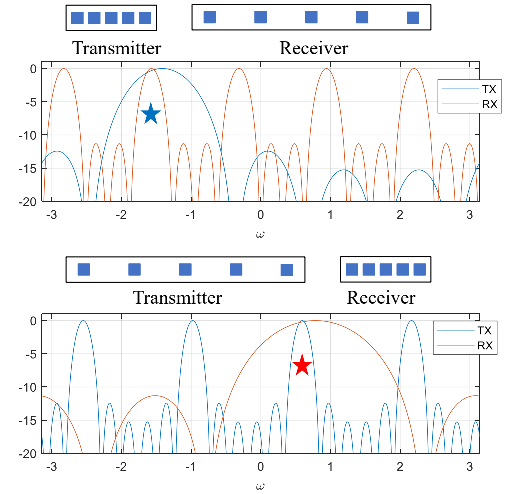

Fig. 3: Spatial undersampling provides aperture extension and improves angular resolution.

II. System Model

We consider a CWFM MIMO radar system which consists of an N_{tx}-element phased array transmitter and an N_{rx}-element, digital receiver, with the frame structure depicted in Figure 2. For each chirp transmission, the return signal at the receiver is mixed with the transmitted chirp and sampled at a rate of B Hz, equivalent to a sampling period of $T_s = 1/B$. The frame is divided into K subframes, each containing a sequence of n_0 chirps. On each subframe, a different randomly-generated beamforming weight vector is applied to form a *compressive beacon*. We use a standard complex Gaussian distribution to draw the beamforming weights, resulting in radiation patterns that spray power randomly in the angular domain, as shown in Figure 2. Thus, in each subframe, the return signal from target t is multiplied by the complex subframe beacon response to spatial frequency

$$\omega_t^{\text{tx}} = \frac{2\pi d_{\text{tx}}}{\lambda} \sin\theta_t \tag{1}$$

where θ_t is the direction of target t, d_{tx} is the transmit array's inter-element spacing, and λ is the carrier wavelength. The target's spatial frequency on the fully digital receiver is derived by taking a spatial FFT and satisfies

$$\omega_t^{\text{rx}} = \frac{2\pi d_{\text{rx}}}{\lambda} \sin\theta_t. \tag{2}$$

We assume here that all targets are sufficiently far away to have AOD = AOA = θ_t.

A. Unambiguous bounds and resolution of parameters

In the system described above, Targets are separated into range, Doppler (radial speed), and spatial frequency bins with a nominal resolution equal to the corresponding FFT grid length of each domain. In evaluating our algorithm, we regard any estimate of range, Doppler, or spatial frequency that lies within one nominal FFT grid length of the true value as a "successful" detection, and any estimate outside this span is considered incorrect. The nominal resolution of each parameter is described as follows.

Range. The minimum and maximum unambiguously measurable range are defined by the receiver sampling rate, B (Hz), and chirp frequency slope, α (Hz/s), as

$$R_{\text{min}} = 0, \quad R_{\text{max}} = \frac{Bc}{2\alpha}$$

where c is the speed of light. The nominal range *resolution* is determined by the length of the chirp. Assuming the system produces L samples per chirp, the range-FFT grid size will be $g_{\text{range}} = 2\pi/L$ equivalent to a nominal range resolution of

$$\delta_R = \frac{R_{\text{max}}}{L} = \frac{Bc}{2\alpha L} = \frac{c}{2\alpha T_{\text{chirp}}}$$

where $T_{\text{chirp}} = LT_s$ is the chirp duration in seconds.

Speed. Similarly, the minimum and maximum unambiguous Doppler measurement is determined by the delay between consecutive chirps. Assuming a duration of T_{gap} between the end of one chirp and the start of the next, the largest Doppler frequency is

$$\frac{\pi}{T_{\text{chirp}} + T_{\text{gap}}},$$

which translates to the radial speed measurement limits,

$$V_{\text{max}} = -V_{\text{min}} = \frac{\lambda}{4(T_{\text{chirp}} + T_{\text{gap}})}.$$

The nominal Doppler FFT grid size is thus equal to

$$\frac{2\pi}{n_0(T_{\text{chirp}} + T_{\text{gap}})}$$

corresponding to nominal radial speed resolution,

$$\delta_V = \frac{\lambda}{2n_0(T_{\text{chirp}} + T_{\text{gap}})} = \frac{\lambda}{2T_{\text{subframe}}},$$

where T_{subframe} is the total subframe duration.

Angle. Unambiguous spatial frequency measurements can be made in the range of $(-\pi, \pi)$ with a grid size of,

$$\delta_{\omega,\text{tx}} = \frac{2\pi}{N_{\text{tx}}}$$

on the transmitter (used for AOD estimation), and

$$\delta_{\omega,\text{rx}} = \frac{2\pi}{N_{\text{rx}}}$$

on the receiver (AOA estimation). These are translated to angular resolution using (1) and (2), respectively as

$$\delta_{\theta,\text{tx/rx}} = \frac{\lambda}{2\pi d_{\text{tx/rx}} \cos\theta}\,\delta_{\omega,\text{tx/rx}}. \tag{3}$$

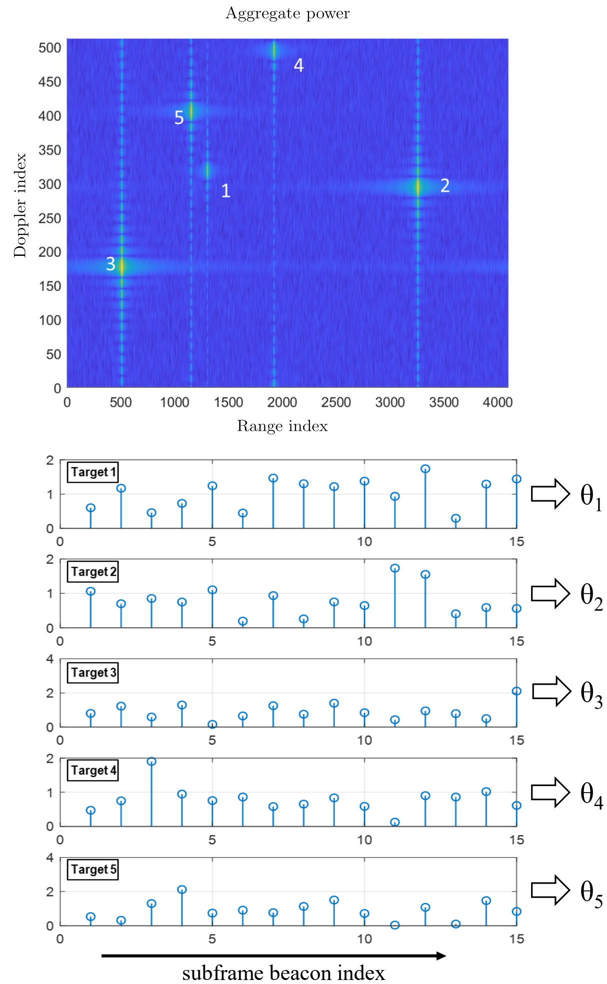

Fig. 4: Aggregated range-Doppler bin powers and compressive direction estimation for a sample scenario.

B. Aperture extension with spatial subsampling

With an appropriate choice of element spacing in the transmitter and receiver, the effective sensing aperture can be increased up to $N_{\text{tx}}N_{\text{rx}}\lambda/2$. Let us assume that the transmitter has half-wavelength spacing while the receiver is spatially undersampled by a factor of N_{tx} (i.e., the inter-element spacing at the receiver is $N_{\text{tx}}\lambda/2$). The translation of transmit spatial frequency to angle is thus the one-to-one transform,

$$\text{AOD} = \sin^{-1}\frac{\omega_{\text{tx}}}{\pi} \tag{4}$$

whereas the undersampled receiver will see "grating lobes" equivalent to the one-to-N_{tx} mapping,

$$\text{AOA} = \sin^{-1}\frac{\omega_{\text{rx}} + 2\pi n}{N_{\text{tx}}\pi}, \quad \exists n \in \{0, ..., N_{\text{tx}} - 1\}. \tag{5}$$

Since AOA = AOD = θ, the angle recovered in (4) can be used to resolve n in (5). Note that the resolution provided by (5) is higher than that of (4) by a factor of (approximately) N_{rx}, meaning the overall direction resolution provided in this way is equivalent to that of an $N_{\text{tx}}N_{\text{rx}}$-element array with half wavelength spacing.

Figure 3 depicts this process of grating lobe resolution from the radiation pattern point of view. Note that the same effect can be achieved by deploying a half-wavelength-spaced *receiver* and spatial undersampling at the *transmitter* by a factor of N_{rx} (also shown in Figure 3).

III. Algorithm

Figure 4 shows a sketch of our proposed imaging process for one frame. This process comprises the following steps.

A. Range-Doppler measurement

In this step, we first take a 2D FFT of each subframe's measurement matrix to arrive at a set of K range-Doppler heatmaps, as shown in Figure 2. By adding up the power in each range-Doppler bin across subframes, we arrive at the "aggregate power heatmap", an example of which is shown in Figure 4. We find the strongest peak in this matrix, obtain an off-grid estimate of its range and Doppler frequency, using a super-resolution technique such as gradient descent, Newton refinements, or local oversampling of the Fourier transform to maximize the aggregate power cost function. We then subtract its response from the measurement matrices of all subframes and proceed to find the next strongest peak in the aggregate power heatmap of the residual response. This process is repeated until no strong peaks relative to the noise floor are observed in the residual heatmap. We denote by N_{bin} the number of extracted bins, and by $\hat{r}_i$ and $\hat{d}_i$the super-resolved range and Doppler frequency estimate of bin i, respectively. In principle, each extracted range-Doppler bin can contain one or more targets, which may be separable in the angular domain. However, when simulating point targets randomly dispersed in the range-Doppler-angle space, this is highly unlikely.

B. Doppler correction and spatial frequency estimation

For each significant bin, we observe a set of K complex amplitudes over the compressive subframes. We denote the observation for bin i on subframe k by y_i^k. In a static setting, this complex amplitude is the sum of the response of compressive beacon k to all the targets inside bin i, and therefore the spatial frequencies of all targets in bin i can be found by using conventional a off-grid compressive estimation algorithm, such as NOPM [9], on the observation vector $\mathbf{y}_i = [y_i^1, ..., y_i^K]^T$. For moving targets, however, the phase of each beacon response is modulated by Doppler drift across subframes, which must be corrected for each subframe measurement to obtain the true compressive spatial projections. For bin i with Doppler frequency d_i, the Doppler phase drift encountered by subframe k is equal to $(k-1)n_0 d_i$. We use our estimate $\hat{d}_i$ to undo this phase offset, and obtain the corrected compressive measurements as

$$\tilde{y}_i^k = y_i^k e^{-j(k-1)n_0 \hat{d}_i}, \quad k = 1, ..., K.$$

The corrected measurement vector $\tilde{\mathbf{y}}_i = [\tilde{y}_i^1, ..., \tilde{y}_i^K]^T$ is used for compressive estimation of the spatial frequencies of targets inside bin i.

Note that, for successful phase correction, the Doppler frequency estimate must be accurate enough to extrapolate well over K subframes, which is why off-grid Doppler estimation in the previous step is crucial for the success of the algorithm.

C. Doppler refinement (optional)

Once a target's direction (spatial frequency) is identified, its compressive beacon response on the K subframes can be calculated. By undoing this spatial beacon response on all subframes, we arrive at an effectively Kn_0-chirp-long subframe that can be used to produce a more accurate off-grid Doppler estimate for that target. This time, instead of using the (noncoherently combined) aggregate power cost function, we can combine likelihoods *coherently* across subframes and achieve higher estimation accuracy relative to our initial estimate.

IV. Numerical Results

In this section, we present simulation results for a MIMO radar system with an $N_{\text{tx}} = 128$ element phased array transmitter with half-wavelength element spacing, and a single-element receiver ($N_{\text{rx}} = 1$). Each frame contains K subframes where K is varied between 5 and 15. Spatial beamforming weights for each subframe are drawn independently from a standard complex Gaussian distribution. Each subframe consists of $n_0 = 32$ chirps, and each chirp of $L = 256$ samples. The distance, radial speed, and direction of targets are drawn randomly such that their corresponding range, Doppler, and spatial frequencies are uniformly distributed over the unambiguous range, save for a single FFT-grid-length gap at each end to prevent wrap-around ambiguity. In each realization, we model 10 targets with 10 dB dynamic range in target signal strengths. Variations in the strength of target responses arises from differences in radar cross section and distance, both of which are modeled in our simulations. The simulation code is available at https://github.com/MaryamRasekh/MIMORadar.

Figure 5 shows the estimation success rate for each parameter as a function of the per-symbol beamformed SNR (which is a factor of N_{tx} higher than the effective SNR for a single-element transmitter) for different values of K. As noted in section II, successful estimation of a parameter implies an absolute estimation error smaller than the nominal FFT grid size. These results are averaged on a per-target basis over 10 realizations, or 100 targets in total. We see that success rate approaches 1 at around -15 dB beamformed SNR, and even with 10 subframes, or 320 chirps per frame, target directions are accurately recovered with the full resolution of a 128-element aperture.

By generating point targets randomly, we are all but guaranteeing that each range-Doppler bin contains at most 1 target, and mutli-target bins are very unlikely to occur. This is likely to be true in real-word systems in all but the zero-Doppler bins where a lot of static clutter is present (assuming, of course, that the radar platform is also static). As a higher number of targets are present in one bin, the number of beacons required to accurately estimate their spatial frequencies will increase

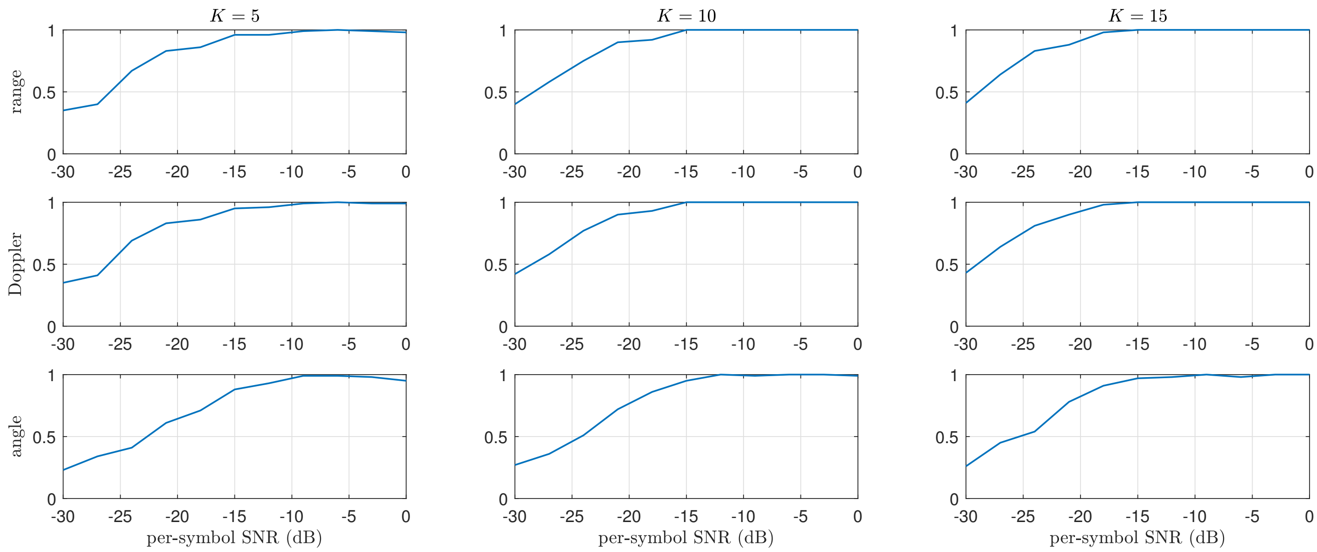

Fig. 5: Success rate of range, Doppler, and angle estimates as a function of SNR and number of subframes K.

proportionally. This is perhaps best managed by generating a new set of compressive beacons for each frame (instead of repeating the same predefined set) so that, by combining several frames, the number of subframe measurements can be adapted to the scene coherence time, and even to the radial speed and number of targets on a per-target or per-bin basis.

V. Conclusions

In this paper, we present a compressive signal processing framework to sidestep the tradeoff between range and field of view that plagues conventional MIMO radar systems. Relying on the angular sparsity of each range-Doppler coordinate of the scene, we take advantage of compressive beam scanning to provide high resolution direction estimates with a small number of beacons that scales logarithmically with array size. The proposed approach enables scaling to massive MIMO frontends while maintaining a small, almost constant frame size, thereby facilitating high resolution direction estimation and range extension without sacrificing the field of view or agility of the imaging system.

Numerical results were presented for simulated point targets on a CWFM radar system with 128 RF-beamformed transmit elements and a single receiver, showing accurate direction estimates are obtained with as few as 10 compressive beacons. In future work, we will investigate the potential for the application of this approach to extended targets with complicated micro-Doppler signatures, and implications for object classification and gesture recognition.

Acknowledgments

This work was supported in part by ComSenTer, one of six centers in JUMP, a Semiconductor Research Corporation (SRC) program sponsored by DARPA.

References

[1] U. Kodak, B. Rupakula, S. Zihir, and G. M. Rebeiz, “A 62 ghz tx/rx 2x128-element dual-polarized dual-beam wafer-scale phased-array transceiver with minimal reticle-to-reticle stitching,” in *2019 IEEE Radio Frequency Integrated Circuits Symposium (RFIC)*. IEEE, 2019, pp. 335–338.

[2] A. Shkel, A. Mehrabani, and J. Kusuma, “A configurable 60ghz phased array platform for multi-link mmwave channel characterization,” in *2021 IEEE International Conference on Communications Workshops (ICC Workshops)*, 2021, pp. 1–6.

[3] S. Krishna, G. Mishra, and S. K. Sharma, “A series fed planar microstrip patch array antenna with 1d beam steering for 5g spectrum massive mimo applications,” in *2018 IEEE Radio and Wireless Symposium (RWS)*, 2018, pp. 209–212.

[4] T. Instruments, “Mimo radar, application report,” *SWRA554A*, May 2017 - revised July 2018.

[5] ——, “Imaging radar using cascaded mmwave sensor reference design,” *Design Guide: TIDEP-01012*, June 2019 - revised March 2020.

[6] Y. Yu, A. P. Petropulu, and H. V. Poor, “Mimo radar using compressive sampling,” *IEEE Journal of Selected Topics in Signal Processing*, vol. 4, no. 1, pp. 146–163, 2010.

[7] Z. Marzi, D. Ramasamy, and U. Madhow, “Compressive channel estimation and tracking for large arrays in mm-wave picocells,” *IEEE Journal of Selected Topics in Signal Processing*, vol. 10, no. 3, pp. 514–527, 2016.

[8] D. Ramasamy, S. Venkateswaran, and U. Madhow, “Compressive adaptation of large steerable arrays,” in *Information Theory and Applications Workshop (ITA), 2012*. IEEE, 2012, pp. 234–239.

[9] B. Mamandipoor, D. Ramasamy, and U. Madhow, “Newtonized orthogonal matching pursuit: Frequency estimation over the continuum,” *arXiv preprint arXiv:1509.01942*, 2015.

[10] Y. Yu, A. P. Petropulu, and H. V. Poor, “Measurement matrix design for compressive sensing–based mimo radar,” *IEEE Transactions on Signal Processing*, vol. 59, no. 11, pp. 5338–5352, 2011.

[11] N. Shahbazi, A. Abbasfar, and M. Jabbarian-Jahromi, “Efficient two-dimensional compressive sensing in mimo radar,” *EURASIP Journal on Advances in Signal Processing*, vol. 2017, no. 1, pp. 1–15, 2017.

[12] M. Rossi, A. M. Haimovich, and Y. C. Eldar, “Spatial compressive sensing for mimo radar,” *IEEE Transactions on Signal Processing*, vol. 62, no. 2, pp. 419–430, 2013.